

# Corneal Vascularization Associated With a Novel *PDGFRB* Variant

Titas Gladkauskas,<sup>1</sup> Ove Bruland,<sup>2</sup> Leen Abu Safieh,<sup>3,4</sup> Deepak P. Edward,<sup>3,5,6</sup> Eyvind Rødahl,<sup>1,7</sup> and Cecilie Bredrup<sup>1,7</sup>

<sup>1</sup>Department of Clinical Medicine, University of Bergen, Bergen, Norway

<sup>2</sup>Department of Medical Genetics, Haukeland University Hospital, Bergen, Norway

<sup>3</sup>Research Department, King Khaled Eye Specialist Hospital, Riyadh, Kingdom of Saudi Arabia

<sup>4</sup>Bioinformatics and Computational Biology Department, Research Center, King Fahad Medical City, Riyadh, Kingdom of Saudi Arabia

<sup>5</sup>Department of Ophthalmology and Visual Sciences, University of Illinois College of Medicine, Chicago, Illinois, United States

<sup>6</sup>Department of Ophthalmology, Loyola University College of Medicine, Chicago, Illinois, United States

<sup>7</sup>Department of Ophthalmology, Haukeland University Hospital, Bergen, Norway

Correspondence: Cecilie Bredrup, Department of Ophthalmology, Haukeland University Hospital, Jonas Lies vei 72, Bergen 5021, Norway; [cecilie.bredrup@helse-bergen.no](mailto:cecilie.bredrup@helse-bergen.no).

Received: April 27, 2023

Accepted: October 16, 2023

Published: November 7, 2023

Citation: Gladkauskas T, Bruland O, Abu Safieh L, Edward DP, Rødahl E, Bredrup C. Corneal vascularization associated with a novel *PDGFRB* variant. *Invest Ophthalmol Vis Sci.* 2023;64(14):9. <https://doi.org/10.1167/iovs.64.14.9>

**PURPOSE.** The purpose of this study was to identify the genetic cause of aggressive corneal vascularization in otherwise healthy children in one family. Further, to study molecular consequences associated with the identified variant and implications for possible treatment.

**METHODS.** Exome sequencing was performed in affected individuals. HeLa cells were transduced with the identified c.1643C>A, p.(Ser548Tyr) variant in the platelet-derived growth factor receptor beta gene (*PDGFRB*) or wild-type *PDGFRB*. ELISA and immunoblot analysis were used to detect the phosphorylation levels of PDGFR $\beta$  and downstream signaling proteins in untreated and ligand-stimulated cells. Sensitivity to various receptor tyrosine kinase inhibitors (TKIs) was determined.

**RESULTS.** A novel c.1643C>A, p.(Ser548Tyr) *PDGFRB* variant was found in affected family members. HeLa cells transduced with this variant did not have increased baseline levels of phosphorylated PDGFR $\beta$ . However, upon stimulation with ligand, excessive activation of PDGFR $\beta$  was observed compared to cells transduced with the wild-type variant. PDGFR $\beta$  with the p.(Ser548Tyr) amino acid substitution was successfully inhibited with tyrosine kinase inhibitors (axitinib, dasatinib, imatinib, and sunitinib) in vitro.

**CONCLUSIONS.** A novel c.1643C>A, p.(Ser548Tyr) *PDGFRB* variant was found in family members with isolated corneal vascularization. Cells transduced with the newly identified variant showed increased phosphorylation of PDGFR $\beta$  upon ligand stimulation. This suggests that PDGF-PDGFR $\beta$  signaling in these patients leads to overactivation of PDGFR $\beta$ , which could lead to abnormal wound healing of the cornea. The examined TKIs prevented such overactivation, introducing the possibility for targeted treatment in these patients.

**Keywords:** hereditary corneal vascularization, *PDGFRB*, activating gene variant, receptor tyrosine kinase inhibitors

In the last decade, several ligand-independent, gain-of-function variants in the platelet-derived growth factor receptor beta gene (*PDGFRB*) have been reported. They have been identified in individuals with a diverse range of disorders. Ocular pterygium digital keloid dysplasia (OPDKD) is associated with a temperature-sensitive, activating p.(Asn666Tyr) substitution in PDGFR $\beta$ .<sup>1</sup> Patients typically develop extensive corneal vascularization in early childhood, followed by development of keloids on the fingers and toes later in life.<sup>1</sup> A more severe phenotype is seen in the Penttinen type of premature aging syndrome, also associated with activating substitutions in PDGFR $\beta$

(p.(Asn666Ser) and p.(Val665Ala)) and in Kosaki overgrowth syndrome (KOGS) linked to the substitutions p.(Pro584Arg), p.(Trp566Arg), p.(Ser493Cys), and p.(Asn856Ile). In these two syndromes, multiple organs are involved. Penttinen syndrome is associated with tissue wasting leading to fragile lipodystrophic skin with ulcerations, acro-osteolysis, and corneal vascularization in early adulthood.<sup>2-5</sup> Kosaki overgrowth syndrome is a somatic overgrowth syndrome characterized by distinctive facial features, accelerated growth with elongated hands and feet, thin and fragile skin, vascularized corneal overgrowth, white matter lesions in the central nervous system (CNS), and developmental delay.<sup>6-11</sup>

It remains unclear why these gain-of-function syndromes are so phenotypically diverse. However, molecular studies on intracellular signaling pathways indicate that each syndrome has a unique pattern of activated downstream signaling proteins.<sup>1-3,5,6,12,13</sup>

Various constitutively active gain-of-function PDGFR $\beta$  substitutions have been successfully targeted with tyrosine kinase inhibitors (TKIs) in in vitro studies.<sup>1,2,5,12,14,15</sup> Several individuals carrying such substitutions have shown clinical improvement when treated with TKIs, typically imatinib.<sup>12,15</sup> Interestingly, an individual with the p.Val665Ala PDGFR $\beta$  substitution exhibited partial clinical improvement with imatinib but showed a more favorable response to dasatinib treatment.<sup>5</sup>

In this report, we describe a novel variant in *PDGFRB*, c.1643C>A, p.(Ser548Tyr), found in 3 family members presenting with aggressive and early-onset corneal vascularization leading to severe visual impairment. In contrast to the other reported *PDGFRB* variants, individuals with the c.1643C>A, p.(Ser548Tyr) variant are otherwise healthy.<sup>16</sup> Although the p.(Ser548Tyr) substitution was not constitutively active, ligand-induced overactivation of PDGFR $\beta$  and downstream signaling were seen after stimulation with platelet-derived growth factor (PDGF). Both ligand-induced overactivation of PDGFR $\beta$  and downstream signaling were inhibited by several TKIs.

## MATERIALS AND METHODS

### Ethical Approval

The Regional Committee for Medical and Health Research Ethics, Western Norway (IRB.no.00001872, project number 2014/59) approved the study. Informed written consent was obtained from affected individuals prior to genetic analysis. The study thus adhered to the Tenets of the Declaration of Helsinki.

### Isolation of DNA, Genotyping, and Exome Sequencing

Blood samples for genotyping were obtained and genomic DNA was isolated. We examined three DNA samples from affected family members (individual II-3, who was legally blind from central corneal scarring with associated peripheral vascularization, and individuals II-1 and III-3).<sup>16</sup> Exome sequencing was performed using the Nextera DNA Library Preparation Kit (Illumina, cat # 15028211) and sequenced on a NextSeq 500 sequencer (Illumina). Variants were called using GenomeAnalysisTK version 3.2-2-gec30cee,<sup>17</sup> following the Broad institute's recommended best practice. Filtration was performed using VCFtools,<sup>18</sup> and annotation of variants was performed using ANNOVAR.<sup>19</sup>

### Transduction of Cells

HeLa cells (ATCC CCL-2) were grown in Dulbecco's Modified Eagle Medium (DMEM) containing 10% fetal calf serum. Transgenic cell preparation was performed as previously described.<sup>2</sup> In brief, a murine retroviral vector containing the *PDGFRB* open-reading frame (NM\_002609.3) was obtained from VectorBuilder. The *PDGFRB* c.wt, c.1996A>T (p.(Asn666Tyr)), or c.1643C>A (p.(Ser548Tyr)) variants were introduced using the QuickChange Site-

Directed Mutagenesis Kit. Virus production was achieved by transfecting Phoenix-AMPHO packaging cells. Two days after transfection, the medium was harvested and HeLa cells were transduced. Two days post-infection, stably transduced cells were selected by adding 1  $\mu$ g/mL puromycin.

### Cell Culture and Stimulation With PDGF

Transduced HeLa cells were seeded in 6-well plates. When the cells were 80% confluent, they were serum-starved for 16 hours and stimulated with PDGF (Platelet-Derived Growth Factor from human platelets; P8147-5UG; Merck KGaA, Darmstadt, Germany; 2.5, 12.5, and 15 ng/mL in 4 mM HCl containing 0.1% BSA) for 20 minutes or with 4 mM HCl containing 0.1% BSA alone as control. According to the manufacturer, the PDGF isolated from platelets consists of approximately 70% PDGF-AB, 20% PDGF-BB, and 10% PDGF-AA. Cells were harvested in 1% NP-40, 20 mM Tris (pH 8.0), 137 mM NaCl, 10% glycerol, 2 mM EDTA, 1 mM activated sodium orthovanadate, 10  $\mu$ g/mL Aprotinin (#4139; Tocris, Abington, United Kingdom), 10  $\mu$ g/mL Leupeptin (Leupeptin hemisulfate, #1167; Tocris, Abington, United Kingdom), and stored at  $-80^{\circ}\text{C}$  until immunoblot or ELISA analysis was performed.

### Reduction of Temperature and Glucose Deprivation

Transduced HeLa cells were either kept at  $37^{\circ}\text{C}$  or incubated overnight at the physiological corneal temperature of  $32^{\circ}\text{C}$ .<sup>20,21</sup> Cells transduced with retroviruses expressing the temperature-sensitive p.(Asn666Tyr) *PDGFRB* variant were used as controls. Cells were harvested as described above.

To examine the effect of glucose deprivation, the medium of the transduced cells was replaced with glucose-free and serum-free DMEM (Thermo Fisher Scientific Inc.; #11966025) for 24 hours.

### Treatment With Receptor Tyrosine Kinase Inhibitors

Three different concentrations were used for treatment with axitinib (AG 013746), dasatinib (BMS-354825), imatinib (STI571), and sunitinib (SU11248) (all purchased from Selleckchem, Munich, Germany). First, we conducted an in-house determination of half-maximal inhibitory concentration ( $\text{IC}_{50}$ ) to evaluate the potency of each drug in our inventory. This was done by stimulating wild-type transduced HeLa cells with PDGF (15 ng/mL), and then determining the drug concentration inhibiting half of the induced PDGFR $\beta$  phosphorylation for each TKI (Supplementary Fig. S1). In addition to these in-house concentrations, we used two other dilutions, including the one recommended by the manufacturer (if available), and the  $\text{IC}_{50}$  concentrations from the review article by Heldin.<sup>22</sup> Transduced HeLa cells serum-starved for 6 hours were treated with axitinib, dasatinib, imatinib, and sunitinib dissolved in DMSO, at these concentrations (see the Table), or with DMSO alone as a control for 6 hours. Cells were stimulated with 12.5 ng/mL PDGF 20 minutes prior to harvesting.

Glucose-deprived cells were treated with axitinib, dasatinib, imatinib, and sunitinib 6 hours prior to harvesting. For

TABLE. Concentrations of the TKIs Used in this Study

Selleckchem	Holdin Literature Review <sup>22</sup>	Titration Studies From This Study
Axitinib	1.6 nM	2 nM
Dasatinib	Not given*	8 nM
Imatinib	380 nM	86 nM
Sunitinib	10 nM	5.6 nM

\* The manufacturer does not give dasatinib IC<sub>50</sub> for PDGFR $\beta$ . Still, the manufacturer states that dasatinib targets Abl, Src, and c-Kit with IC<sub>50</sub> of <1 nM, 0.8 nM, and 79 nM in cell-free assays, respectively. In this study, we used 100 nM dasatinib as previously described.<sup>5</sup>

this experiment, only TKI concentrations from the in-house titration study were used.

### ELISA and Immunoblot Analysis

ELISA and immunoblot analyses were performed as previously described.<sup>2</sup> In brief, ELISA analysis was conducted using a DuoSet IC PDGFR $\beta$  kit (#DYC1767-2, R&D systems) in accordance with the guidelines provided by the manufacturer. In this kit, the total phosphorylation levels of PDGFR $\beta$  are measured using an immobilized antibody binding PDGFR $\beta$  and an HRP-conjugated antibody against phosphorylated tyrosine. For immunoblot analysis, protein separation was carried out using a high-resolution gel system (4–12% NuPAGE Novex Bis-Tris Gel; Life, Carlsbad, CA, USA) following the manufacturer's instructions and transferred to nitrocellulose membranes (Bio-Rad, Hercules, CA, USA). Membranes were blocked with 5% non-fat dry milk (Bio-Rad), 1% glycine, and 1% BSA in PBS-T buffer (standard PBS with 0.05% Tween 20). They were incubated overnight at 4°C with primary antibodies from Cell Signalling Technology (Danvers, MA, USA) used at recommended dilutions (catalogue numbers in parentheses): phospho-Tyr70-STAT1 (#7649), STAT1 (#9172), phospho-Tyr783-PLC $\gamma$ 1 (#2821), PLC $\gamma$ 1 (#5690), phospho-Ser473-AKT (#4060), phospho-AKTThr308 (#4056), AKT (#4691), phospho-38 MAPK (Thr180/Tyr182; #9211), phospho-Thr202/Tyr204-MAPK3/ERK1 (#4370), and MAPK3/ERK1 (#4695). To control for equal loading, anti-GAPDH antibodies (Sigma #G99545) were used. ImageJ software was used for relative quantification of immunoblot band intensity.

### Statistical Analysis and Reproducibility

Paired *t*-test was performed to compare PDGFR $\beta$  phosphorylation levels measured with ELISA. All results were replicated in at least three independent experiments. Representative images are shown in the figures.

## RESULTS

### Clinical Examination

The family has been described previously.<sup>16</sup> To summarize, aggressive corneal changes diagnosed as pterygium with extension across the visual axis appeared early in life in three otherwise healthy family members (individuals II-1, III-2, and III-3). In addition, individual II-3 had central corneal scarring with associated peripheral vascularization, and individual III-6 had dense corneal opacity, lateral rectus palsy, and unilateral horizontal nystagmus (Fig. 1).

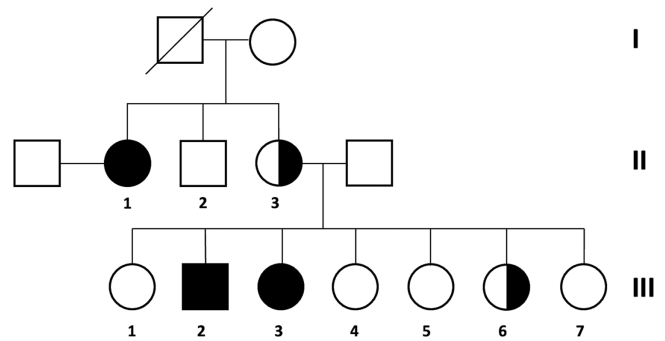


FIGURE 1. Pedigree indicating affected family members. Individuals II-1, III-2, and III-3 developed pterygium in the early 20s, and at 6, and 4 years of age, respectively (*fully-shaded symbols*). Individuals II-1 and III-3 had a unilateral pterygium, whereas bilateral pterygium was seen in III-2. Individual II-3 was declared legally blind from central corneal scarring with associated peripheral vascularization, and III-6 had severe visual impairment due to dense corneal opacity in the left eye (*half-shaded symbols*). Individuals II-1, II-3, and III-3 were included in this study. The clinical data are summarized in the supplementary materials (Supplementary Table S1).

### A Novel PDGFRB Variant

Exome sequencing revealed a variant in *PDGFRB*, NM\_002609.3: c.1643C>A, p.(Ser548Tyr) shared by all 3 affected individuals. This previously unreported variant is absent in gnomAD, dbSNP, and other variant databases. Additionally, it has not been detected in in-house samples subjected to exome sequencing at the Department of Medical Genetics, Haukeland University Hospital, Bergen, Norway. The missense variant changes a highly conserved amino acid located in the transmembrane domain of PDGFR $\beta$  (Supplementary Fig. S2). There is a major physicochemical difference between Ser and Tyr, and the variant was predicted to be damaging by SIFT and MutationTaster.

### The PDGFR $\beta$ p.(Ser548Tyr) Substitution Does Not Cause Ligand-Independent Auto-Activation

In HeLa cells stably transduced with either the c.1643C>A, p.(Ser548Tyr), or wild-type *PDGFRB* vector, similar levels of both PDGFR $\beta$  and phosphorylated PDGFR $\beta$  were observed (Fig. 2A, Supplementary Fig. S3). In line with this, comparable phosphorylation levels of the examined PDGFR $\beta$  downstream signaling proteins (p-AKT<sup>Ser473</sup>, p-AKT<sup>Tyr308</sup>, p-PLC $\gamma$ 1, p-MAPK3/ERK1, and p-STAT1) were found (Fig. 2B). This indicates that the p.(Ser548Tyr) substitution is not causing constitutive ligand-independent auto-activation of PDGFR $\beta$ .

### The PDGFR $\beta$ p.(Ser548Tyr) Substitution Causes Ligand-Dependent Over-Activation

When p.(Ser548Tyr) cells were stimulated with 2.5 or 12.5 ng/mL PDGF, increased levels of phosphorylated PDGFR $\beta$  (see Fig. 2A) were seen compared to wild-type cells, with a 2.2 and 1.9 fold increase, respectively. This indicated that the p.(Ser548Tyr) amino acid substitution leads to excessive PDGFR $\beta$  activation upon ligand binding.

We next examined downstream signaling proteins after ligand stimulation. Although comparable levels of p-STAT1 were found in p.(Ser 548Tyr) and wild-type cells, increased

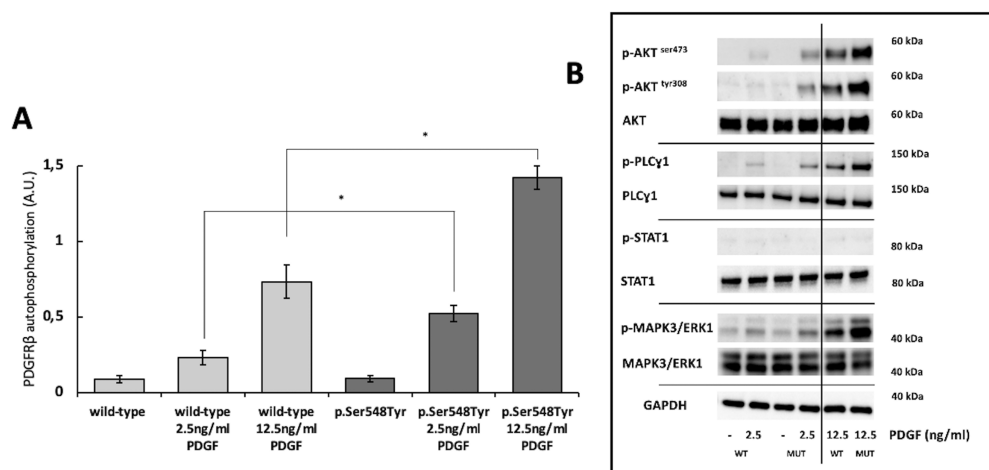


**FIGURE 2.** (A) Levels of phosphorylated PDGFR $\beta$  measured by ELISA analysis. The untreated wild-type and p.(Ser548Tyr) cells have comparable PDGFR $\beta$  phosphorylation levels. Upon stimulation with PDGF (2.5 ng/mL and 12.5 ng/mL), higher PDGFR $\beta$  phosphorylation levels were found in p.(Ser548Tyr) cells. Data are shown as mean  $\pm$  SEM of three independent experiments. Paired *t*-test was performed to compare wild-type and p.(Ser548Tyr) response to PDGF stimulation, \*  $P < 0.01$ . (B) Representative images showing effect of ligand stimulation on PDGFR $\beta$  downstream signaling proteins. Increased levels of downstream signaling proteins, p-AKT<sup>Ser473</sup>, p-AKT<sup>Tyr308</sup>, and p-PLC $\gamma$ 1 upon PDGF stimulation were seen in p.(Ser548Tyr) cells, whereas no such effect was seen on p-STAT1. Upon stimulation with low levels of PDGF, comparable levels of p-MAPK3/ERK1 were found, whereas at high concentration (12.5 ng/mL) increased phosphorylation levels were observed in p.(Ser548Tyr) cells. The p-AKT<sup>Ser473</sup>/GAPDH, p-AKT<sup>Tyr308</sup>/GAPDH, and p-PLC  $\gamma$ 1/GAPDH ratios upon stimulation with 2.5 ng/mL PDGF were 4.9, 12.8, and 3.7 folds higher in p.(Ser548Tyr) cells compared to wild-type cells. All results were replicated in at least three independent experiments. ELISA analysis data point distributions, full immunoblottings, and quantification of representative images are shown in Supplementary Figures S4 and S5.

phosphorylation of p-AKT<sup>Ser473</sup>, p-AKT<sup>Tyr308</sup>, and p-PLC $\gamma$ 1, were present in cells expressing the p.(Ser548Tyr) substitution (see Fig. 2B) at both ligand concentrations. For phospho-Thr202/Tyr-MAPK3/ERK1, a different pattern was seen. Here, comparable levels were present upon stimulation with low ligand concentration (2.5 ng/mL) in both cell types, whereas stimulation with 12.5 ng/mL PDGF led to higher levels in p.(Ser548Tyr) cells.

### The PDGFR $\beta$ p.(Ser548Tyr) Substitution is not Temperature Sensitive but is Responsive to Glucose Deprivation

Upon prolonged glucose withdrawal (24 hours), increased levels of p-AKT<sup>Ser473</sup> were observed in p.(Ser548Tyr) cells compared to wild-type cells (Fig. 3). No difference in phosphorylation of PDGFR $\beta$  or downstream signaling protein p-AKT<sup>Tyr308</sup>, p-PLC $\gamma$ 1, p-ERK1/2, and p-STAT1 was found (Supplementary Fig. S6). Comparable phosphorylation levels of PDGFR $\beta$  and downstream signaling partners were observed for p.(Ser548Tyr) and wild-type cells upon exposure to the corneal physiological temperature of 32<sup>o</sup>20.21 (Supplementary Fig. S7).

### Tyrosine Kinase Inhibitors Inhibit the PDGFR $\beta$ p.(Ser548Tyr) Ligand-Dependent Over-Activation

All the examined TKIs (axitinib, dasatinib, imatinib, and sunitinib) inhibited the ligand-induced activation of PDGFR $\beta$  and its downstream signaling partners both in p.(Ser548Tyr) and wild-type cells (Fig. 4). Of these, axitinib at both 1.6 nM and 2 nM concentrations reduced the phosphorylated PDGFR $\beta$  by 4.2 to 5-fold. This was more effective

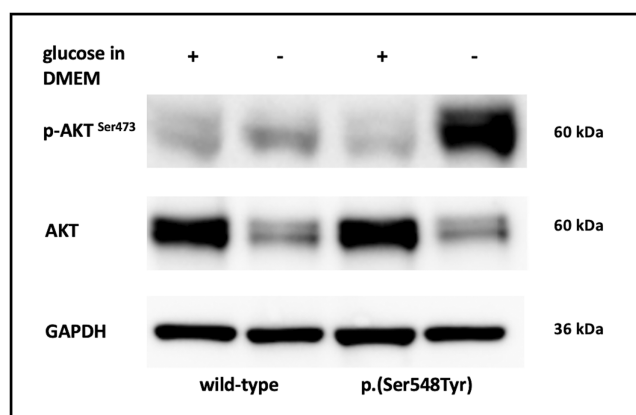


**FIGURE 3.** Representative images showing immunoblot analysis of AKT, p-AKT<sup>Ser473</sup>, and GAPDH in wild type cells and cells expressing the p.(Ser548Tyr) substitution cultivated with and without glucose. The p-AKT<sup>Ser473</sup>/GAPDH ratio in p.(Ser548Tyr) cells after glucose withdrawal compared with wild-type cells after glucose withdrawal, and with p.(Ser548Tyr) cells under normal glucose conditions was 5.8 folds and 14 folds higher, respectively. All results were replicated in at least three independent experiments. Full immunoblotting and quantification of representative images are shown in Supplementary Figure S6.

than imatinib achieving 1.3 and 2.5-fold reduction, respectively, at comparable concentrations (86 nM and 380 nM). Sunitinib and dasatinib reduced activation ranging from 1.8 to 5.2 and 1.5 to 5.4 fold, respectively (see Fig. 4A).

The increased levels of p-AKT<sup>Ser473</sup> seen upon glucose withdrawal were also inhibited with all tested TKIs (Supplementary Fig. S8).

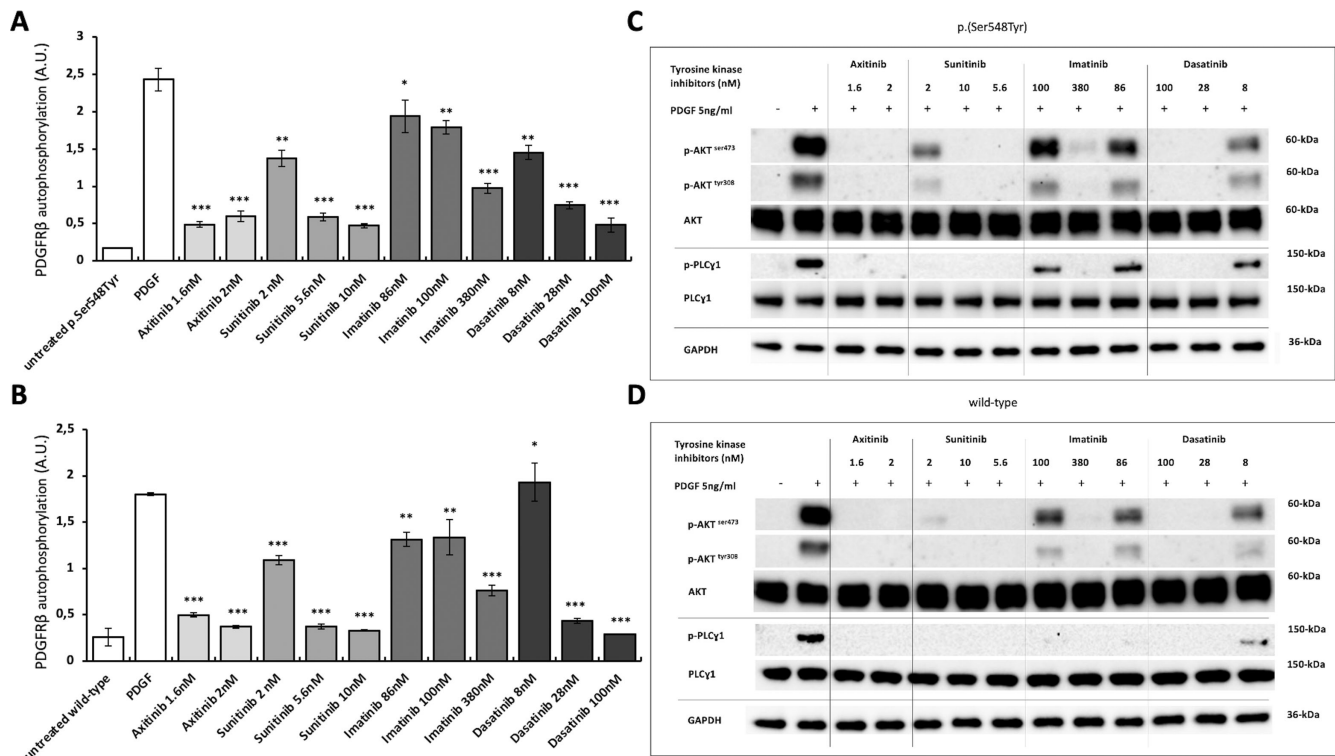


**FIGURE 4.** Effect of tyrosine kinase inhibitors on PDGFR $\beta$  and downstream signaling proteins. Panels (A) and (B) show ligand-induced PDGFR $\beta$  autophosphorylation levels measured with ELISA in p.(Ser548Tyr) (A) and wild type (B) cells after incubation with four tyrosine kinase inhibitors (axitinib, dasatinib, imatinib, and sunitinib) at different concentrations. Data are shown as mean  $\pm$  SEM of three independent experiments. Paired *t*-test was performed to compare drug effect on PDGF-stimulated PDGFR $\beta$ . \*  $P < 0.05$ , \*\*  $P < 0.01$ , and \*\*\*  $P < 0.001$ . Panels (C) and (D) show representative images of immunoblot analysis of downstream signaling proteins in p.(Ser548Tyr) (C) and wild-type (D) cells after incubation with tyrosine kinase inhibitors at different concentrations. Axitinib, at all used concentrations, most effectively inhibited phosphorylated PDGF/PDGFR $\beta$  and downstream signaling cascades. All results were replicated in at least three independent experiments. ELISA analysis data point distributions, full immunoblottings, and quantification of representative images are shown in Supplementary Figures S9 to S11.

## DISCUSSION

PDGF is an extracellular signaling molecule with a vital role during embryonal development, hematopoiesis, and wound healing.<sup>23–25</sup> Together with factors like BMP2, BMP4, and IL-1 $\alpha$ , PDGF signaling plays a crucial role in fibroblast chemotaxis and proliferation, influencing corneal health and injury recovery.<sup>26</sup> PDGF binds to PDGFR $\alpha$  and PDGFR $\beta$ , two receptor tyrosine kinases (RTKs) with a nearly identical domain structure, including five extracellular immunoglobulin (Ig) loops, a helical transmembrane domain, a juxtamembrane region, and a split intracellular tyrosine kinase (TK) domain. After stimulation with PDGF, dimerization of PDGFRs triggers an auto-catalyzed trans-phosphorylation in the intracellular domain.<sup>27</sup> The receptors' phosphorylated tyrosine residues become specific docking platforms to recruit SH2 or PTB domains containing effector proteins.

In members of a family presenting with early-onset corneal vascularization, we found a novel missense variant in *PDGFRB*, c.1643C>A, p.(Ser548Tyr). The variant is located in exon 11, leading to a p.(Ser548Tyr) substitution in the PDGFR $\beta$  transmembrane domain. This exon is highly conserved among various animal species (see Supplementary Fig. S2). Patients carrying the p.(Ser548Tyr) substitution have similar corneal changes as patients with OPDKD.<sup>1</sup> The corneal overgrowth is more aggressive than what has been

reported in Penttinen type of premature aging syndrome<sup>2,5</sup> and Kosaki overgrowth syndrome.<sup>8,9</sup> These diseases are all caused by *PDGFRB* variants leading to ligand-independent activation of the kinase.

It has been shown that the transmembrane (TM) domain of RTKs contributes to the stability of full-length dimers. Thus, this part of the kinase is thought to be important for maintaining a signaling-competent dimeric receptor conformation.<sup>28–30</sup> There is a broad spectrum of phenotypes in human diseases arising from disease-causing substitutions in the TM domain of various RTKs.<sup>29</sup> It has been suggested that these substitutions can activate RTKs by several mechanisms, such as by altering dimerization, ligand binding, or phosphorylation.<sup>31</sup> We observed ligand-induced overactivation of PDGFR $\beta$  and downstream signaling proteins (see Fig. 2), possibly due to altered phosphorylation of the kinase caused by the p.(Ser548Tyr) substitution.

In contrast to the previously reported *PDGFRB* variants, we found that the p.(Ser548Tyr) substitution is not causing constitutive ligand-independent activation (see Fig. 2). Instead, the p.(Ser548Tyr) substitution caused ligand-dependent PDGFR $\beta$  overactivation. (see Fig. 2A). In line with this, upregulation of downstream signaling proteins, AKT<sup>Tyr308</sup>, AKT<sup>Ser473</sup>, and PLC $\gamma$ 1, were found upon ligand stimulation (see Fig. 2B). The cornea is constantly exposed to minor traumas/scratches,<sup>32,33</sup> which can lead to the

secretion of PDGF.<sup>34,35</sup> Although speculative, individuals carrying the *PDGFRB* p.(Ser548Tyr) variant may have an excessive wound healing response to such minor corneal traumas, in turn leading to corneal vascularization. Details on the ocular microenvironment, such as the tear film, meibomian gland function, and the lid margins were not described in the case report<sup>16</sup> but may be relevant for the observed phenotype.

The avascular cornea has unique environmental conditions, such as a low physiological temperature (30–32°C) and low glucose levels.<sup>36–45</sup> A temperature-sensitive mutation in *PDGFRB*, p.(Asn666Tyr) is associated with corneal vascularization.<sup>1</sup> Such a response to the physiological corneal temperature was not found in p.(Ser548Tyr) cells. Glucose starvation, however, caused an upregulation of p-AKT<sup>Ser473</sup> (see Fig. 3), in p.(Ser548Tyr) cells. Graham and co-workers described that glucose withdrawal may initiate a positive feedback loop involving the generation of reactive oxygen species and inhibition of protein tyrosine phosphatases by oxidation, hence increasing tyrosine kinase signaling.<sup>46</sup> However, the precise mechanism behind the observed increase in AKT signaling upon glucose starvation remains to be elucidated.

AKT and PLCY1 phosphorylation have important roles in PDGFR $\beta$  ligand-induced cell proliferation, differentiation, survival, growth, migration, and angiogenesis.<sup>47–49</sup> Interestingly, the AKT signaling pathway is important for the effect of PDGFR $\beta$  p.(Asn666Tyr) associated with OPDKD, suggesting that it is important for the corneal overgrowth phenotype. In contrast, increased STAT1 signaling has been linked to tissue wasting,<sup>50</sup> among others in Penttinen syndrome.<sup>2,5,13</sup> Our affected family members have no degenerative features and in line with this, no STAT1 upregulation was observed (see Fig. 2B).

Individuals with activating mutations in *PDGFRB* are candidates for treatment with TKIs, with imatinib being the most widely used.<sup>1,2,5,12–15</sup> However, recent studies with various gain-of-function variants in *PDGFRB* suggest that there are differences in the sensitivity to various TKIs.<sup>5,12–14</sup> When examining different TKIs (axitinib, dasatinib, imatinib, and sunitinib), we observed that all four TKIs inhibited PDGFR $\beta$  activation in ligand-stimulated p.(Ser548Tyr), wild-type cells (see Fig. 4) and upregulated p-AKT<sup>Ser473</sup> after glucose deprivation (see Supplementary Fig. S8). In addition, variation in the potency of the TKIs at different concentrations was observed (see Fig. 4), with axitinib being somewhat more effective in inhibiting ligand-induced PDGFR $\beta$  phosphorylation. By using the most potent drug, clinicians could titrate the lowest drug dosage within the therapeutic window minimizing risks of side effects of the TKIs.<sup>51</sup>

Alternative treatment options for gain-of-function *PDGFRB* variants may include anti-PDGF antibodies or antibody-drug conjugates.<sup>52,53</sup> A number of additional approaches for treating corneal vascularization are being explored, from targeting the VEGF-pathway to stem cell transplantation.<sup>54–56</sup> Further research is required to decide the best treatment options for gain-of-function *PDGFRB* variants leading to corneal overgrowth.

In summary, we present a novel *PDGFRB* p.(Ser548Tyr) variant associated with severe corneal vascularization. The substitution leads to ligand-dependent overactivation of the kinase and downstream signaling, in particular AKT signaling. Targeted treatment using TKIs might be an option in patient treatment.

## Acknowledgments

The authors would like to thank Unni Larsen for technical assistance.

Supported by grants from the Western Norway Regional Health Authority (911977 and 912161 to C.B.), Gidske og Peter Jacob Sørensen Forskningsfond (to T.G.), Olav Raaholt og Gerd Meidel Raagholt's stiftelsen (to T.G.), and Futura Fund for scientific medical research (to C.B.).

Disclosure: **T. Gladkauskas**, None; **O. Bruland**, None; **L. Abu Safieh**, None; **D.P. Edward**, None; **E. Rødahl**, None; **C. Bredrup**, None

## References

- Bredrup C, Cristea I, Safieh LA, et al. Temperature-dependent autoactivation associated with clinical variability of PDGFRB Asn666 substitutions. *Hum Mol Genet*. Published online January 15, 2021:ddab014, doi:10.1093/hmg/ddab014.
- Bredrup C, Stokowy T, McGaughran J, et al. A tyrosine kinase-activating variant Asn666Ser in PDGFRB causes a progeria-like condition in the severe end of Penttinen syndrome. *Eur J Hum Genet*. 2019;27(4):574–581.
- Johnston JJ, Sanchez-Contreras MY, Keppler-Noreuil KM, et al. A point mutation in PDGFRB causes autosomal-dominant Penttinen syndrome. *Am J Hum Genet*. 2015;97(3):465–474.
- Aggarwal B, Correa ARE, Gupta N, Jana M, Kabra M. First case report of Penttinen syndrome from India. *Am J Med Genet A*. 2022;188(2):683–687.
- Iznardo H, Bredrup C, Bernal S, et al. Clinical and molecular response to dasatinib in an adult patient with Penttinen syndrome. *Am J Med Genet A*. Published online December 11, 2021:ajmg.a.62603, doi:10.1002/ajmg.a.62603.
- Zarate YA, Boccuto L, Srikanth S, et al. Constitutive activation of the PI3K-AKT pathway and cardiovascular abnormalities in an individual with Kosaki overgrowth syndrome. *Am J Med Genet A*. 2019;179(6):1047–1052.
- Minatogawa M, Takenouchi T, Tsuyusaki Y, et al. Expansion of the phenotype of Kosaki overgrowth syndrome. *Am J Med Genet A*. 2017;173(9):2422–2427.
- Foster A, Chalot B, Antoniadi T, et al. Kosaki overgrowth syndrome: a novel pathogenic variant in PDGFRB and expansion of the phenotype including cerebrovascular complications. *Clin Genet*. 2020;98(1):19–31.
- Mutlu Albayrak H, Calder AD. Kosaki overgrowth syndrome: report of a family with a novel PDGFRB variant. *Mol Syndromol*. Published online September 29, 2021:1–7, doi:10.1159/000517978.
- Takenouchi T, Yamaguchi Y, Tanikawa A, Kosaki R, Okano H, Kosaki K. Novel overgrowth syndrome phenotype due to recurrent de novo PDGFRB mutation. *J Pediatr*. 2015;166(2):483–486.
- Gawliński P, Pelc M, Ciara E, et al. Phenotype expansion and development in Kosaki overgrowth syndrome. *Clin Genet*. 2018;93(4):919–924.
- Rustad CF, Tveten K, Prescott TE, Bjerkeseth PO, Bredrup C, Pfeiffer HCV. Positive response to imatinib in PDGFRB-related Kosaki overgrowth syndrome. *Am J Med Genet A*. 2021;185(8):2597–2601.
- Nédélec A, Guérit EM, Dachy G, et al. Penttinen syndrome-associated PDGFRB Val665Ala variant causes aberrant constitutive STAT1 signalling. *J Cell Mol Med*. 2022;26(14):3902–3912.
- Arts FA, Chand D, Pecquet C, et al. PDGFRB mutants found in patients with familial infantile myofibromatosis or over-

- growth syndrome are oncogenic and sensitive to imatinib. *Oncogene*. 2016;35(25):3239–3248.
15. Pond D, Arts FA, Mendelsohn NJ, Demoulin JB, Scharer G, Messinger Y. A patient with germ-line gain-of-function PDGFRB p.N666H mutation and marked clinical response to imatinib. *Genet Med*. 2018;20(1):142–150.
  16. Islam SI, Wagoner MD. Pterygium in young members of one family. *Cornea*. 2001;20(7):708–710.
  17. McKenna A, Hanna M, Banks E, et al. The genome analysis toolkit: a MapReduce framework for analyzing next-generation DNA sequencing data. *Genome Res*. 2010;20(9):1297–1303.
  18. Danecsek P, Auton A, Abecasis G, et al. The variant call format and VCFtools. *Bioinformatics*. 2011;27(15):2156–2158.
  19. Wang K, Li M, Hakonarson H. ANNOVAR: functional annotation of genetic variants from high-throughput sequencing data. *Nucleic Acids Res*. 2010;38(16):e164.
  20. Slettedal JK, Ringvold A. Correlation between corneal and ambient temperature with particular focus on polar conditions. *Acta Ophthalmol (Copenh)*. 2015;93(5):422–426.
  21. Kessel L, Johnson L, Arvidsson H, Larsen M. The relationship between body and ambient temperature and corneal temperature. *Invest Ophthalmol Vis Sci*. 2010;51(12):6593.
  22. Heldin CH. Targeting the PDGF signaling pathway in the treatment of non-malignant diseases. *J Neuroimmune Pharmacol*. 2014;9(2):69–79.
  23. Andrae J, Gallini R, Betsholtz C. Role of platelet-derived growth factors in physiology and medicine. *Genes Dev*. 2008;22(10):1276–1312.
  24. Pierce GF, Mustoe TA, Altmann BW, Deuel TF, Thomason A. Role of platelet-derived growth factor in wound healing. *J Cell Biochem*. 1991;45(4):319–326.
  25. Gao Z, Sasaoka T, Fujimori T, et al. Deletion of the PDGFR- $\beta$  gene affects key fibroblast functions important for wound healing. *J Biol Chem*. 2005;280(10):9375–9389.
  26. Kim WJ, Mohan RR, Mohan RR, Wilson SE. Effect of PDGF, IL-1 $\alpha$ , and BMP2/4 on corneal fibroblast chemotaxis: expression of the platelet-derived growth factor system in the cornea. *Invest Ophthalmol Vis Sci*. 1999;40(7):1364–1372.
  27. Kelly JD, Haldeman BA, Grant FJ, et al. Platelet-derived growth factor (PDGF) stimulates PDGF receptor subunit dimerization and intersubunit trans-phosphorylation. *J Biol Chem*. 1991;266(14):8987–8992.
  28. Bocharov EV, Mineev KS, Volynsky PE, et al. Spatial structure of the dimeric transmembrane domain of the growth factor receptor ErbB2 presumably corresponding to the receptor active state. *J Biol Chem*. 2008;283(11):6950–6956.
  29. Li E, Hristova K. Role of receptor tyrosine kinase transmembrane domains in cell signaling and human pathologies. *Biochemistry*. 2006;45(20):6241–6251.
  30. Li E, Hristova K. Receptor tyrosine kinase transmembrane domains: function, dimer structure and dimerization energetics. *Cell Adhes Migr*. 2010;4(2):249–254.
  31. He L, Hristova K. Physical–chemical principles underlying RTK activation, and their implications for human disease. *Biochim Biophys Acta BBA - Biomembr*. 2012;1818(4):995–1005.
  32. Sun D, Gong L, Xie J, et al. Toxicity of silicon dioxide nanoparticles with varying sizes on the cornea and protein corona as a strategy for therapy. *Sci Bull*. 2018;63(14):907–916.
  33. Kashiwagi K, Iizuka Y. Effect and underlying mechanisms of airborne particulate matter 2.5 (PM<sub>2.5</sub>) on cultured human corneal epithelial cells. *Sci Rep*. 2020;10(1):19516.
  34. Vesaluoma M, Teppo AM, Grönhagen-Riska C, Tervo T. Platelet-derived growth factor-BB (PDGF-BB) in tear fluid: a potential modulator of corneal wound healing following photorefractive keratectomy. *Curr Eye Res*. 1997;16(8):825–831.
  35. Hoppenreijns VP, Pels E, Vrensen GF, Treffers WF. Effects of platelet-derived growth factor on endothelial wound healing of human corneas. *Invest Ophthalmol Vis Sci*. 1994;35(1):150–161.
  36. Cohen GY, Ben-David G, Singer R, et al. Ocular surface temperature: characterization in a large cohort of healthy human eyes and correlations to systemic cardiovascular risk factors. *Diagnostics*. 2021;11(10):1877.
  37. Yang WL, Zhang L. Normal range of temperature of cornea on ocular surface of healthy people in Pudong New District of Shanghai. *J Shanghai Jiaotong Univ Med Sci*. 2010;30:832–834.
  38. Cejková J, Stípek S, Crkovská J, et al. UV rays, the prooxidant/antioxidant imbalance in the cornea and oxidative eye damage. *Physiol Res*. 2004;53(1):1–10.
  39. Delic NC, Lyons JG, Di Girolamo N, Halliday GM. Damaging effects of ultraviolet radiation on the cornea. *Photochem Photobiol*. 2017;93(4):920–929.
  40. Thoft RA. Corneal glucose concentration: flux in the presence and absence of epithelium. *Arch Ophthalmol*. 1971;85(4):467.
  41. Turss R, Friend J, Reim M, Dohlman CH. Glucose concentration and hydration of the corneal stroma. *Ophthalmic Res*. 1971;2(5):253–260.
  42. McCarey BE, Schmidt FH. Modeling glucose distribution in the cornea. *Curr Eye Res*. 1990;9(11):1025–1039.
  43. Domingo E, Moshirfar M, Zabbo CP. Corneal abrasion. In: *StatPearls*. Treasure Island, FL: StatPearls Publishing; 2021.
  44. Li X, Kang B, Eom Y, et al. Comparison of cytotoxicity effects induced by four different types of nanoparticles in human corneal and conjunctival epithelial cells. *Sci Rep*. 2022;12(1):155.
  45. Xiang P, He RW, Han YH, Sun HJ, Cui XY, Ma LQ. Mechanisms of housedust-induced toxicity in primary human corneal epithelial cells: oxidative stress, proinflammatory response and mitochondrial dysfunction. *Environ Int*. 2016;89–90:30–37.
  46. Graham NA, Tahmasian M, Kohli B, et al. Glucose deprivation activates a metabolic and signaling amplification loop leading to cell death. *Mol Syst Biol*. 2012;8(1):589.
  47. Caglayan E, Vantler M, Leppänen O, et al. Disruption of platelet-derived growth factor–dependent phosphatidylinositol 3-kinase and phospholipase C $\gamma$  1 activity abolishes vascular smooth muscle cell proliferation and migration and attenuates neointima formation in vivo. *J Am Coll Cardiol*. 2011;57(25):2527–2538.
  48. Manning BD, Toker A. AKT/PKB signaling: navigating the network. *Cell*. 2017;169(3):381–405.
  49. Hajicek N, Keith NC, Siraliev-Perez E, et al. Structural basis for the activation of PLC- $\gamma$  isozymes by phosphorylation and cancer-associated mutations. *eLife*. 2019;8:e51700.
  50. He C, Medley SC, Kim J, et al. STAT1 modulates tissue wasting or overgrowth downstream from PDGFR $\beta$ . *Genes Dev*. 2017;31(16):1666–1678.
  51. Hartmann J, Haap M, Kopp HG, Lipp HP. Tyrosine kinase inhibitors – a review on pharmacology, metabolism and side effects. *Curr Drug Metab*. 2009;10(5):470–481.
  52. Chen L, Wu H, Ren C, et al. Inhibition of PDGF-BB reduces alkali-induced corneal neovascularization in mice. *Mol Med Rep*. 2021;23(4):238.
  53. Lee SJ, Kim S, Jo DH, et al. Specific ablation of PDGFR $\beta$ -overexpressing pericytes with antibody-drug conjugate potently inhibits pathologic ocular neovascularization in mouse models. *Commun Med*. 2021;1(1):58.

54. Chang JH, Garg NK, Lunde E, Han KY, Jain S, Azar DT. Corneal neovascularization: an anti-VEGF therapy review. *Surv Ophthalmol.* 2012;57(5):415–429.
55. Yazdanpanah G, Haq Z, Kang K, Jabbehdari S, Rosenblatt ML, Djalilian AR. Strategies for reconstructing the limbal stem cell niche. *Ocul Surf.* 2019;17(2):230–240.
56. Lee JY, Knight RJ, Deng SX. Future regenerative therapies for corneal disease. *Curr Opin Ophthalmol.* 2023;34(3):267–272.